

Steady-State and Time Resolved Fluorescence Analysis on Tyrosine–Histidine Model Compounds

Mariana Voicescu · Martine Heinrich · Petra Hellwig

Received: 13 June 2008 / Accepted: 11 August 2008 / Published online: 3 September 2008
© Springer Science + Business Media, LLC 2008

Abstract Four model compounds, for a tyrosine–histidine covalent bonding, 2-(5-imidazolyl)-4-methylphenol (C–C bonding in *ortho*-position at the phenyl group); 2'-(1-imidazolyl)-4-methylphenol (C–N bonding in *ortho*'-position at the phenyl group); 2-(5-imidazolyl)-4-H-phenol and 2-(5-imidazolyl)-4-H-phenol, at physiological pH have been studied by UV-Vis absorption, steady-state and time resolved fluorescence spectroscopy. Their absorption and emission properties are presented and discussed. The photophysical properties depend on the *para*-substituted phenyl group as well as on C–C/C–N bonding in the Phenol–Imidazole linkage. The N position, *N1–N3/N1–N4*, in the imidazole group was found to be relevant. The results are discussed with relevance to the redox processes of tyrosine and to better understand the role of a tyrosine–histidine covalent linkage as found in cytochrome *c* oxidase.

Keywords Tyrosine–histidine model compounds · Cytochrome *c* oxidase · UV absorbance · Fluorescence lifetime

Introduction

Fluorescence spectroscopy is a useful technique for studies on the dynamics of conformational changes in proteins. Tyrosine is one of three naturally occurring amino acids besides Phenylalanine and tryptophan that contributes to ultraviolet fluorescence [1]. Tyrosine emission in water occurs at 303 nm and is relatively insensitive towards solvent polarity. Tyrosine is often regarded as a simple fluorophore. In the case of the tyrosine zwitterion and tyrosine derivatives with an ionized carboxyl group, mono-exponential fluorescence decay is reported, with a fluorescence lifetime of about 3.3–3.4 ns [2, 3] and with a fluorescence quantum yield equal to 0.14. It was found that after the incorporation of tyrosine into a peptide chain, its fluorescence quantum yield decreases, whereas the fluorescence intensity decay becomes heterogeneous [1, 2]. Also, the conversion of the tyrosine carboxyl group or analogues of the corresponding amide causes the quenching of their fluorescence. The influence of the conversion of a carboxyl group into an amide group or the amino group into the *N*-acetyl group of tyrosine or of its analogues on their photophysical properties was widely investigated [4, 5].

The fluorescence quenching mechanism of tyrosine derivatives is based on the dependence of the quenching efficiency on the distance between the phenol group of the tyrosine residue and its amide group [5]. Furthermore the dependence of the electron transfer rate constant on the ionization potential of the excited fluorophore was found for a series of amidated tyrosine analogues and their derivatives [4]. Amino group acetylation of tyrosine or its analogues causes a moderately decreased fluorescence quantum yield and fluorescence lifetime, the fluorescence intensity decay, however, is still mono-exponential [2]. The methylation of the hydroxyl group on the phenol ring of the tyrosine increases both, the

M. Voicescu · M. Heinrich · P. Hellwig
Laboratoire de Spectroscopie Vibratoire
et Electrochimie des Biomolécules,
UMR 7177, Institut de Chimie,
CNRS-Université Louis Pasteur, 1 rue Blaise Pascal,
67070 Strasbourg, France

M. Voicescu (✉)
Romanian Academy,
Institute of Physical Chemistry “Ilie Murgulescu”,
Splaiul Independentei 202,
060021 Bucharest, Romania
e-mail: mvoicescu@chimie.u-strasbg.fr

fluorescence quantum yield and the fluorescence lifetime as compared to tyrosine, but does not change the character of the fluorescence intensity decay of tyrosine itself as well as the amide or *N*-acetyl derivative [2, 5].

The influence of the pH on the fluorescence of tyrosine, tryptophan and related compounds was studied by White [6]. The protonation of the tyrosine carboxyl group decreases the fluorescence quantum yield [7] and the fluorescence lifetime [8, 9]. In the pH range from 4 to 8, the fluorescence quantum yield of tyrosine is constant and the decay is mono-exponential with a lifetime of about 3.4 ns. This indicates that the excited-state proton transfer from phenol hydroxyl to water, though thermodynamically allowed, is too slow to affect the fluorescence decay [2, 10]. For pH > 8, the fluorescence quantum yield decreases, while the fluorescence lifetime remains constant due to the tyrosinate formation; Tyrosinate presents a negligible fluorescence [11, 12]. The pK_a value of the carboxyl group of the 3-(4-hydroxy)-propionic acid, an analogue of tyrosine devoid of an amino group, is 4.5 [10] or 4.9 [13], which indicates that the presence of the protonated amino group has a strong influence on the acid–base properties of the carboxyl group. A direct interaction between the carbonyl group and the phenol ring, resulting in quenching of the excited state and lowering the pK_a of the carboxyl group of tyrosine in the excited state was suggested by Pal et al. [8] and Fayet and Whal [12]. Based on differences between pK_a values in the ground and excited states for tyrosine isomers (*o*-, *m* and *p*-tyrosine), Pal et al. [8] suggested that the interaction of the carboxyl group with the chromophore via the hydroxyl group of the phenol ring exists in the excited state.

Recently, the acidity of the carboxyl group of Tyr and its analogues and derivatives was investigated by steady state fluorescence spectroscopy [7], revealing that the methylation of the hydroxyl group of the phenol ring, as well as the position of the carboxyl group with respect to the phenol ring (tyrosine, β -tyrosine), had a minor influence on the value of pK_a . The introduction of an additional hydroxyl group into a phenol ring (Dopa) slightly increased the acidity of the carboxyl group compared to tyrosine, whereas the replacement of the α -H atom in Dopa by an α -methyl group caused an increase of the pK_a compared to the value observed for tyrosine [7]. The photophysical properties of tyrosine at low pH range were also investigated [14] and it was found by global analysis of the fluorescence intensity decay of tyrosine at different pH values that the quenching of tyrosine fluorescence by H_3O^+ ions is connected to the presence of a protonated carboxyl group.

A fluorescence study concerning tryptophan–histidine interactions in the anantin peptide and in solution [15] showed that imidazole is a better quencher in the protonated

form, and that the nature of the solvent is involved even in the quenching by unprotonated imidazole.

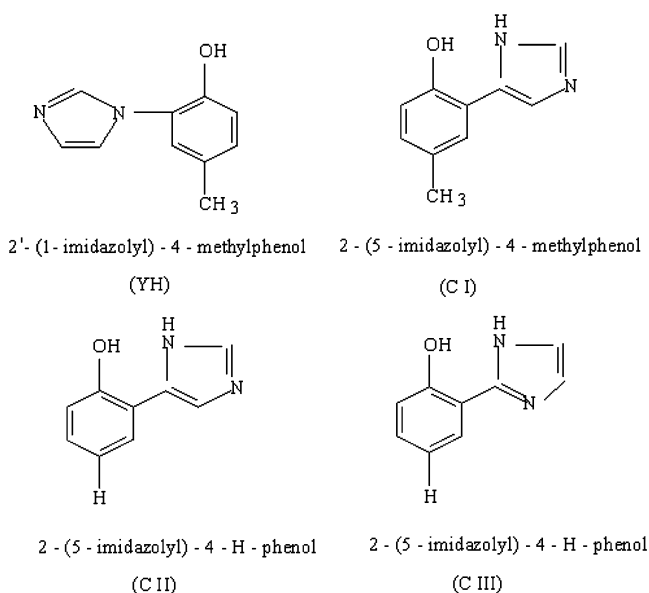
The current paper deals with the spectrophotometric characterization (absorption and fluorescence) of four model compounds with a covalently linked tyrosine–histidine, studied at physiological pH. Their spectral and kinetic properties caused by *para*-substituted phenyl group as well as the influence of C–C/C–N bonding in phenol–imidazole linkage and of the N position in the imidazole group on the above mentioned properties have been investigated. The relevance of the results for tyrosine redox processes and for Tyr–His covalent linkage in proteins will be discussed [16].

Experimental

Materials The structure of the studied compounds is shown in Scheme 1. The compounds were synthesized by the research team of Dr. van der Donk, Illinois, USA [16]. The solutions were prepared in 20 mM Tris–HCl Buffer, pH 7.4. Tris (hydroxymethylaminomethan) was purchased from Sigma-Aldrich. The pH was measured using a Microprocessor pH-Meter, Model pH 211, from HANNA Instruments. Ludox, AS-40 Colloidal Silica, 40 wt% suspension in water, was purchased from Sigma-Aldrich.

Methods and apparatus

The absorption measurements were recorded at room temperature using a CARY 300 SCAN, UV-VIS Spectrometer (Varian). The spectrometer parameters were: average



Scheme 1 The molecular structure of the investigated Tyr–His model compounds

time, 0.1 s; date interval, 1 nm; scan rate, 600 nm/min; SBW, 2 nm; beam mode, double. The final concentration of the compounds was 5×10^{-5} M.

The fluorescence emission spectra were recorded with a Fluorolog FL3-22 equipped with a 450 W Xenon Lamp and a TBX 04 detector (Horiba Jobin Yvon), using 5 nm bandpasses for the excitation and the emission monochromators, increment of 1 nm for the emission monochromator, integration times of 0.1 s. The emission spectra were corrected for the lamp, the monochromators and the detector response. The excitation wavelength was 275 nm and the compound concentration 3×10^{-5} M. The fluorescence quantum yields, ϕ , were determined according to the method of Parker and Ress [17],

$$\phi_x = (F_x A_{\text{ref}} \phi_{\text{ref}}) / F_{\text{ref}} A_x$$

where F is the area under the fluorescence emission curve, for Trp (F_{ref}) and for the studied compound (F_x) over the wavelength region 290–450 nm, A_{ref} is the absorbance for Trp at 295 nm, and the quantum yield ϕ_{ref} for Trp in H_2O is taken as 0.12 [18].

Fluorescence quenching of Tyr with imidazole (Im) The fluorescence intensity F as a function of the quencher concentration $[Q]$ is fitted by the classical Stern–Volmer equation:

$$F_0/F = 1 + K_{\text{SV}}[Q],$$

where F_0 and F represent the fluorescence intensities in the absence and, respectively, in the presence of the quencher; K_{SV} is the Stern–Volmer quenching constant ($K_{\text{SV}} = k_q \times \tau_0$, where k_q is the rate constant of the bimolecular quenching process, τ_0 is the fluorescence lifetime in the absence of the quencher), and $[Q]$ is the quencher molar concentration [1].

The fluorescence decays for Tyr and Tyr–His model compounds were collected by time-correlated single-photon counting (TCSPC) technique. The excitation source was an electroluminescent diode (NanoLED-295, Horiba Jobin Yvon) emitting at 295 nm with a bandwidth of about 12 nm and giving pulses of about 730 ps full width half maximum. The NanoLED diode operated at 1 MHz repetition rate, Coaxial delay 70 ns, TAC Range 50 ns, 14.5 nm band pass. The decay curves were stored in 1,024 channels of 0.056 ns per channel. The NanoLED pulse was recorded using a diluted Ludox solution (0.01%). The concentration of the compounds was 3×10^{-5} M and all measurements were performed at 20°C. To determine the fluorescence lifetime of the compounds, the fluorescence

decay data were fitted by a single-, double-, or a triple exponential function

$$F(t) = \alpha_1 \exp(-t/\tau_1) + \alpha_2 \exp(-t/\tau_2) + \alpha_3 \exp(-t/\tau_3)$$

using Decay Analysis Software with reconvolution (DAS6), from Horiba Jovin Yvon.

The data were fitted using nonlinear least squares methods [19]. The quality of the data fit was judged using statistical parameters and graphical tests. The reduced chi-squared values were close to 1. The weighed residuals were low and uniformly distributed around zero. $\langle \tau \rangle$, the average fluorescence lifetimes were calculated from the following relation: $\langle \tau \rangle = \sum \alpha_i \tau_i^2 / \sum \alpha_i \tau_i$ [1].

In all fluorescence measurements, solutions were placed into a 10 mm precision cell made of special optical glass for fluorescence, the final working volume being of 1,000 μl .

FTIR/electrochemical analysis The spectroelectrochemical cell [20] was used for FTIR measurements in the 2,000 to 1,000 cm^{-1} spectral region equipped with calcium fluoride windows. A gold grid was used as the working electrode; it was chemically modified with a 2 mM cysteamine solution for 1 h and then washed with distilled water [21]. The counter and reference electrodes were a Pt wire and an Ag/AgCl sat 3 M KCl electrode, respectively. The working electrode was then set in the cell, and pushed against the window to form a thin layer of solution (about 10 μm). A potential step of 0–0.7 V was applied (vs. Ag/AgCl/3 M KCl); add+ 0.208 V for the standard hydrogen electrode (SHE') potentials. The sample solutions were prepared in 20 mM Tris–HCl, pH 7.4 and KCl added to a final concentration of 100 mM. The FTIR spectrometer (Bruker IFS 28) was equipped with a DTGS detector. Scanner velocity was 10 kHz and six times 256 scans were averaged at a resolution of 4 cm^{-1} . The measurements were performed at 5°C, using a water thermostat. Electrochemically induced difference spectra were recorded and processed as previously described by Hellwig et al. [21].

Results and discussion

UV-Vis absorption measurements

The studied compounds, although relatively similar in molecular structure, exhibit clear differences in their experimental UV-Vis absorption spectra by variations of the shape and position of characteristic bands. Figure 1 shows the absorption spectra of YH and C I model compounds, at 5×10^{-5} M in 20 mM Tris–HCl pH 7.4, in the spectral range 200–375 nm, in direct comparison to Tyr

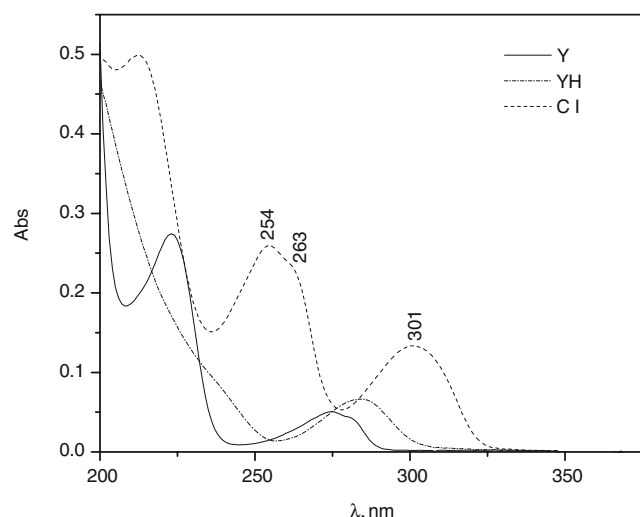


Fig. 1 Absorption spectra of 5×10^{-5} M Tyr–His model compounds in 20 mM Tris–HCl buffer, pH 7.4

spectrum. Two electronic bands are evident: at 237 (shoulder) and 283 nm—for the YH compound, at 254 and 301 nm, for the C I compound. The absorption spectra of YH and C I model compounds are broader and red-shifted (bathochromic shift). The absorption maxima of the four Tyr–His model compounds at physiological pH and the corresponding molar extinction coefficients, ϵ , are summarized in Table 1.

The influence of the C–C and C–N bondings, in phenol–imidazole linkage, on the absorption spectra of the Tyr–His model compounds are considered. The maximum of the absorption spectrum of Tyr in 20 mM Tris–HCl pH 7.4 is 274 nm, whereas for the absorption spectra of the YH model compound it is 283 nm. For the C I model compound, with a C–C bonding phenol–imidazole, the absorption maximum displayed an additional red-shift (18 nm). Moreover, a shoulder at 263 nm is observed. Thus, the replacement of the C–N with a C–C bonding in the phenol–imidazole linkage seems to have an influence on the position of the maximum of the absorption spectrum and on the shape of the band. The ϵ value for the C I compound is higher than the ϵ value of the YH compound (Table 1).

Para-methyl substitution at the Phenol ring by H-atom Due to the planarity of the phenyl ring, as proven by DFT calculations [22], the replacement of the methyl group (YH and C I model compounds) by a hydrogen atom (the case of the C II and C III model compounds) extends the conjugation of the π -electrons from the imidazole ring to the benzene ring. A bathochromic shift between C II and C III model compounds of $\Delta_{\max} \sim 6$ nm for the low-energy band ($S_0 \rightarrow S_1^*$ transition), is evident. One can observe that for the C III compound a more intense shoulder occurs at 273 nm and another absorption band at 345 nm is observed.

It can be noticed that the position of the absorbance maxima is characteristic for each Tyr–His model compound and subsequently bathochromic shifts are induced by deprotonation of the phenol hydroxyl group, process that differently takes place as a function of the model compound.

Thus, the influence of *para*-methyl substitution at the phenol ring as well as the C–N/C–C bonding, in phenol–imidazole linkage, reduces the extension of conjugation, and a shift of the long wavelength absorption band, from 301 nm (C I) to 283 nm (YH) is observed. For the YH model compound the shoulder at 237 nm is characteristic for the anion state and assigned to the La ($^1B_{1u}$) transition of *para*-substituted phenol. We note that, this could also be due to the overlapping of the vibrational bands.

The N position in the imidazole group also induces spectral modifications. In the case of the C III compound (with the N1–N4 position of N), Scheme 1, the low energy band is red-shifted and the influence on the ϵ values is high (Table 1). For this model compound, an absorption band at 345 nm appears.

Comparing all studied Tyr–His model compounds, one can conclude that *para*-methyl substituted phenyl groups (YH and C I compounds) and *para*-H substituted phenyl groups (C II and C III compounds) as well as the N position at the imidazole ring (N1–N3 in YH, C I, C II compounds and N1–N4 in the C III compound) play an important role in the distribution of energy in the

Table 1 Absorption (λ_{Abs} and ϵ), emission (λ_{em} and fluorescence quantum yield [ϕ_f]) and Stokes shift ($\Delta\nu$) of Tyr–His model compounds, in 20 mM Tris–HCl buffer, pH 7.4

Compound	λ_{Abs} (nm)	$\epsilon \times 10^3$ ($l \text{ M}^{-1} \text{ cm}^{-1}$)	λ_{em} (nm)	$\Delta\nu$ (cm^{-1})	ϕ_f
Y	223	1.0	304	3,357	0.14 ^a
	274				
YH	237 (sh)	1.2	328	4,568	0.08
	283				
C I	212	2.6	330	3,012	0.12
	254				
	263 (sh)				
C II	301	1.4	330	3,549	0.10
	210				
	254				
C III	262 (sh)	3.6	334	3,236	0.06
	295				
	213				
	263				
	273 (sh)				
	301		405		
	345				

The compound concentration is 5×10^{-5} M in absorption and 3×10^{-5} M in fluorescence, $\lambda_{\text{ex}} = 275$ nm

^a Value from R.F. Chen [18]

absorption spectra, evidenced by bathochromic shifts and increased ϵ values. Modifications of the ϵ values (higher values for C III) are observed when comparing all the studied compounds: The red-shift observed for the absorption spectra of all Tyr–His model compounds in direct comparison to that of the free Tyr, indicates that the lower energy absorption band of Tyr shows an electronic structure that is lost upon ionization of the phenol hydroxyl group. Moreover, the shift of the maximum of the absorption spectra of Tyr–His model compounds in direct comparison to free Tyr, could be a marker for Tyr–His containing proteins.

Steady-state fluorescence measurements

All four Tyr–His model compounds are fluorescent, with high quantum yield values (Table 1), thus being interesting for studies on intrinsic fluorescence in proteins.

The influence of C–C/C–N bonding in phenol–imidazole linkage

Fluorescence emission spectra of Tyr and Tyr–His model compounds are shown in Fig. 2a. YH and C I have emission spectra consisting of one structured band, at 328 and 330 nm respectively, red-shifted by comparison to the emission band of free Tyr, at 304 nm. These red-shifted emissions could cover the wavelength region that includes tyrosinate fluorescence, which has a maximum near 350 nm [11]. On the other hand these red-shifted emissions could be induced by the H-bonding of the phenol hydroxyl group. Table 1 shows the positions of the emission maxima (λ_{em}) in the fluorescence spectra of YH and C I model compounds. The fluorescence intensity of the C I compound is higher than that of the YH compound and the wavelength emission is slightly red shifted (2 nm). The fluorescence intensity of the YH compound is extensively broadened, due to the overlapping of the vibrational bands. The shoulders in the emission spectrum of the YH compound were better defined by decomposing the spectrum in five Gaussian bands: at 24,878 cm^{-1} , 27,453, 29,501, 31,292 and 32,653 cm^{-1} , respectively (Fig. 2b). The difference of the behavior of the YH model compounds on the excited state can be also observed in larger Stokes Shift ($\Delta\nu=4,568 \text{ cm}^{-1}$), comparatively with free Tyr ($\Delta\nu=3,357 \text{ cm}^{-1}$) as well as with the other Tyr–His model compounds: C I ($\Delta\nu=3,012 \text{ cm}^{-1}$), C II ($\Delta\nu=3,549 \text{ cm}^{-1}$) and C III ($\Delta\nu=3,236 \text{ cm}^{-1}$) respectively, Table 1. This is an indication that YH model compound has a different geometry on the excited state by comparison to that of the ground state. In Fig. 3 the spectral distribution of absorption and emission intensities of the C III model compound are presented. The fluorescence

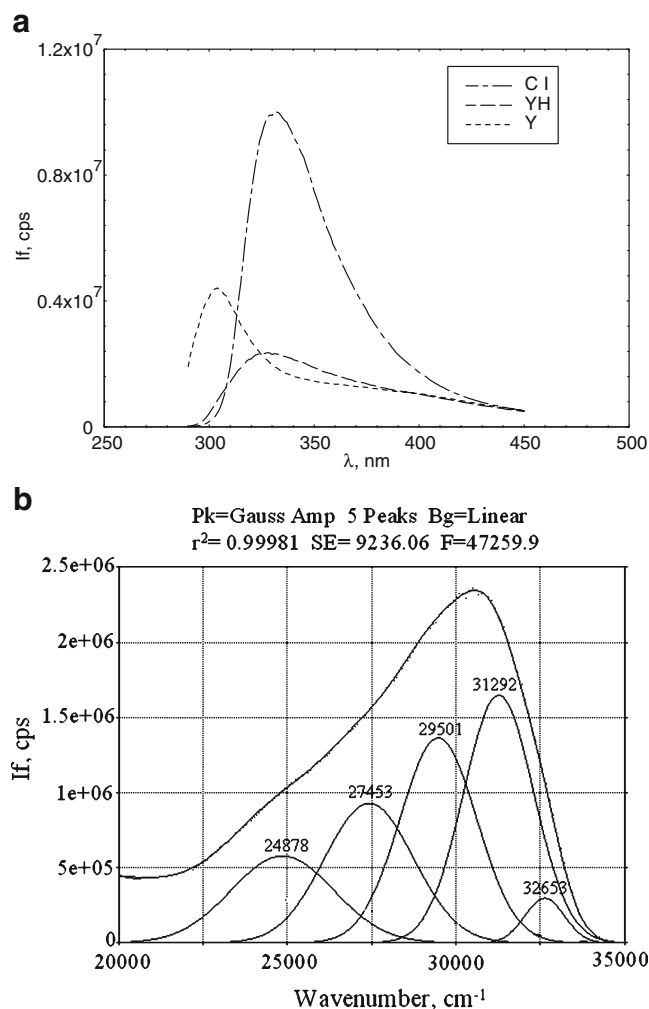


Fig. 2 Fluorescence emission spectra of 3×10^{-5} M in 20 mM Tris–HCl buffer pH 7.4 of the YH and C I model compounds; $\lambda_{ex}=275$ nm (a) and deconvolution of the emission spectrum of the YH model compound (b)

quantum yield of the C I model compound was found to be higher than that of the YH model compound.

The effect of para-substituted phenyl group and N position in the imidazole group

Table 1 presents the differences observed in the fluorescence emission between C II and C III Tyr–His model compounds. The emission spectrum of the C III compound, Fig. 3, has two emission maxima, at 334 and 405 nm and the fluorescence intensity decreases by comparison with the C II compound. These modifications are due to para-methyl substitution at the phenol ring by H atom, as well as to N position at the imidazole ring, position that in the case of the C III compound could better favor the extension of the π electrons conjugation. The second emission band, at 405 nm, can be attributed to Tyr phosphorescence. That means that the Tyr side of the C III molecular structure is

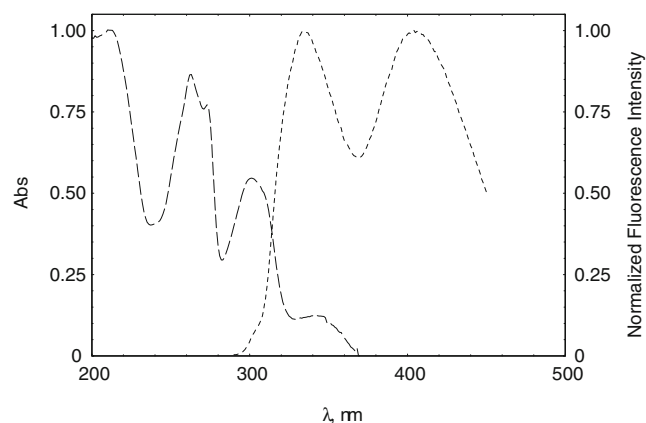


Fig. 3 The normalized absorption and emission spectra in 20 mM Tris-HCl buffer pH 7.4 of the CIII model compound

shielded from collisions. The fluorescence quantum yield of this compound decreases (Table 1) probably due to internal proton transfer.

Tyr fluorescence quenching by imidazole

Figure 4a shows the fluorescence emission spectra of Tyr in the presence of Im. It was found that in the presence of Im, the Tyr fluorescence intensity significantly decreases. This variation can be correlated with the increase of Im concentration. The Tyr fluorescence quenching by Im can be attributed to a dynamic process, analyzed by the Stern–Volmer equation. The variation F_0/F versus molar quencher concentration is linear, Fig. 4b, and from the slope, the Stern–Volmer, K_{SV} , constant was obtained. The bimolecular extinction rate constant, k_q , of the process was calculated, considering the excited-state lifetime of the Tyr fluorescence, τ_0 , being 3.25 ns (Table 2). Values of $K_{SV}=22 \text{ M}^{-1}$ and $k_q=0.68 \times 10^{10} \text{ M}^{-1}\text{s}^{-1}$ were obtained, indicating that Tyr is accessible to quenching by Im. It is known that for Tyr, and small Tyr-containing peptides, the values of k_q are near $1.2 \times 10^{10} \text{ M}^{-1}\text{s}^{-1}$ [23, 24].

The second emission band that appears at 376 nm, without shifting the wavelength, is attributed to Tyrosinate formation. The excited-state proton transfer from Tyr to Im takes place, and because the tyrosinate is only weakly fluorescent [25], this ionization effectively quenches the emission from Tyr. Im is a better quencher in the protonated than in the unprotonated form. This may be explained by the formation of a nonfluorescent charge transfer complex between indole and Im [15, 26].

On this basis, the value of k_q is of interest because it reflects the collisional frequency of the fluorophore with a quencher and subsequently, the extent to which the Tyr residue in a Tyr–His containing protein is shielded from

such collisions by the surrounding protein. Thus, for Tyr residues embedded into a protein, the measured value of k_q indicates the rate at which the quencher molecule penetrates the protein.

Time-resolved fluorescence measurements

The values for fluorescence decay of the Tyr–His model compounds investigated, the lifetime and the pre-exponential values, are presented in Table 2. After deconvolution, a monoexponential (in the case of C I, C II and C III compounds) or a triple exponential (in the case of YH compound) decay curve is obtained. In this later case, three conformers in the excited state may co-exist. The presented pre-exponential values α_1 , α_2 and α_3 give evidence to the fraction of the total fluorescence intensity

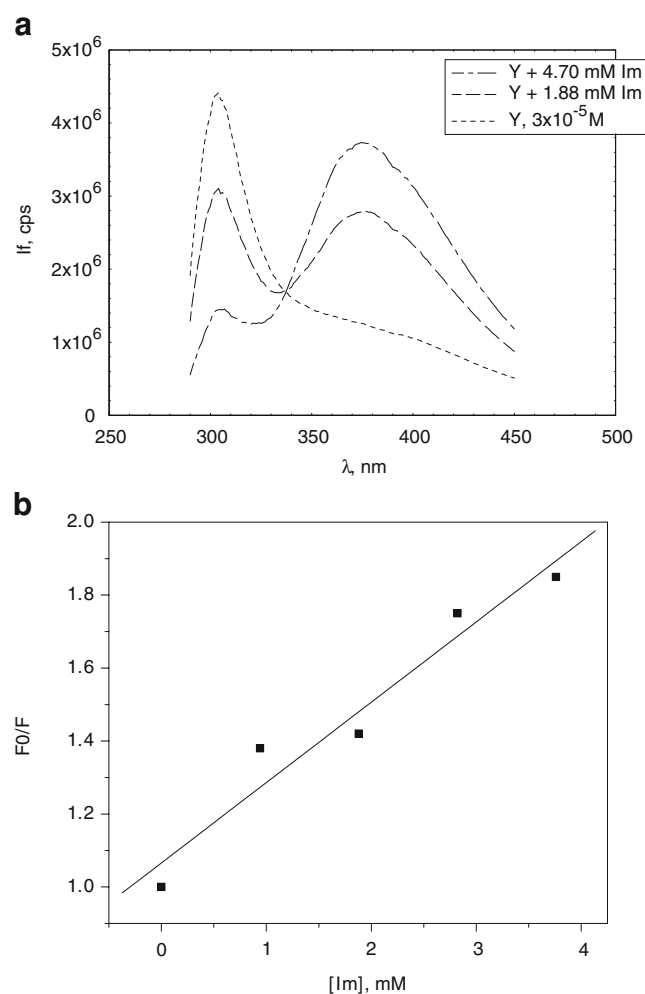


Fig. 4 Fluorescence emission spectra of $3 \times 10^{-5} \text{ M}$ in 20 mM Tris-HCl buffer pH 7.4 of Tyr in the presence of imidazole; $\lambda_{\text{ex}}=275 \text{ nm}$ (a) and Stern–Volmer plot of the fluorescence intensity of Tyr as a function of Imidazole concentration (b)

Table 2 Fluorescence lifetimes and pre-exponential factors of YH model compounds in 20 mM Tris–HCl buffer, pH 7.4

Compound	τ_1 (ns)	α_1	τ_2 (ns)	α_2	τ_3 (ns)	α_3	$\langle\tau\rangle$ (ns)	χR^2
Y _{aq}	1.07	0.0270	3.52	0.8390	0.16	0.1339	3.47	1.04
Y	0.023	0.5863	3.31	0.4137	–	–	3.25	1.16
YH	0.12	0.3212	0.62	0.6237	4.53	0.0551	2.03	0.99
C I	2.66	1.0000	–	–	–	–	2.66	0.95
C II	2.48	1.0000	–	–	–	–	2.48	1.30
C III	1.58	1.0000	–	–	–	–	1.58	1.28

The compound concentration is 3×10^{-5} M; $\lambda_{\text{ex}}=295$ nm; χR^2 presents the quality of the fit; the residuals goodness of the fit values were determined for 1-, 2- and 3-component fits. Y_{aq} is Tyr in aqueous solution

relative to each conformer. From Table 2 it can be observed that $\alpha_2 > \alpha_3$, thus the fraction of intensity related to the slow component of the fluorescence decay is higher than that of the fast component. Moreover, the lifetime components found in the order of 100 ps are compatible with the reorientation of small chromophoric molecules.

Figure 5 is shown as an example for the fluorescence decay curves ($\lambda_{\text{em}}=320$ nm) of YH (Fig. 5a) and C I (Fig. 5b) compounds and the random distributions of weighted residuals (standard deviations). The fluorescence lifetime values, τ , for all studied Tyr–His model compounds are lower than the fluorescence lifetime value of free Tyr. Here, 3.25 ns value have been found. It is known that Tyr has a fluorescence decay time, $\tau=3.38$ ns [10]. Moreover, fluorescence lifetime and quantum yield for Tyr incorporated into a protein strongly depend on micro surrounding and rotamers population [2, 27]. One can observe that for the C III compound, the τ value is smaller (1.58 ns) in comparison with the τ value of C II (2.48 ns), due to the extension of the π -electron conjugation. For the C I compound, the τ value is higher, 2.66 ns. This could be explained by the fact that the molecular structure of C I is better involved in the hydrogen bonds formation, thus the stability of the compound to the UV radiation during the lifetime measurement is higher. In the Scheme 2, the position of the H-bond in the C I model compound is presented. Moreover, the monoexponential fluorescence intensity decays of C I, C II and C III Tyr–His model compounds could support the role of the H-bonds. Due to the *para*-substituted phenol ring by a hydrogen atom (which could give more stability) the hydroxyl group of the C II and C III model compounds is less involved in forming a strong H-bond. Guzew et al. [28] found that the fluorescence decay of Tyr derivatives in acetonitrile solution is monoexponential and, in contrast to the aqueous solution, the amide group does not quench the fluorescence. Thus, specific conformations stabilized by H-bonds are responsible for the heterogeneous fluorescence intensity decay of Tyr derivatives in aqueous solution [28].

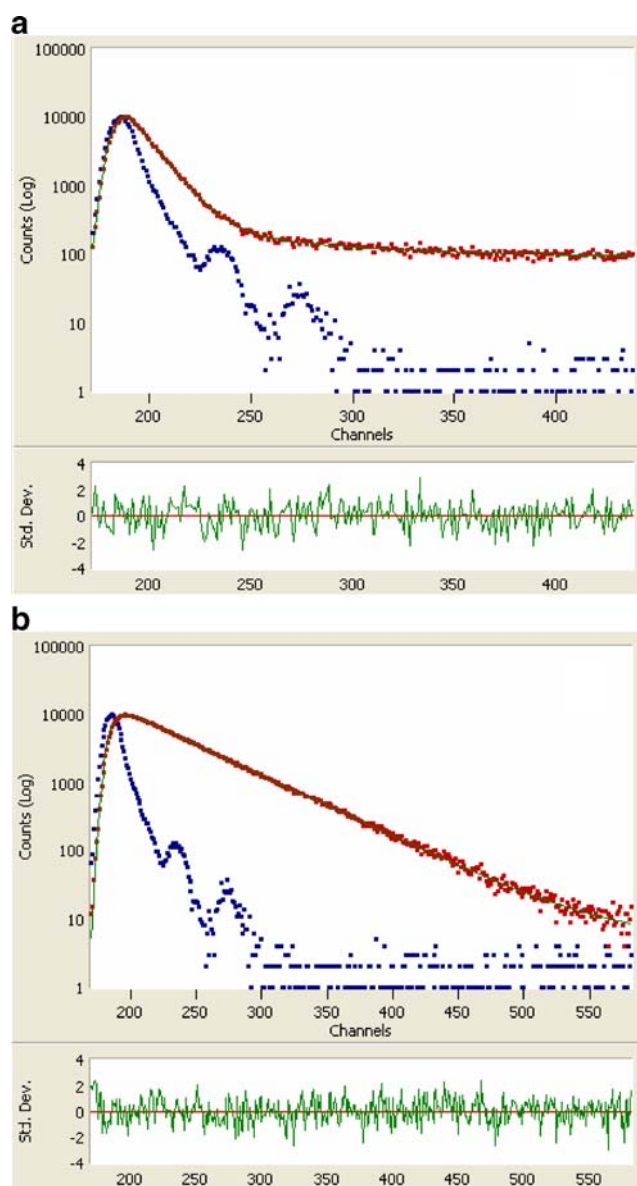
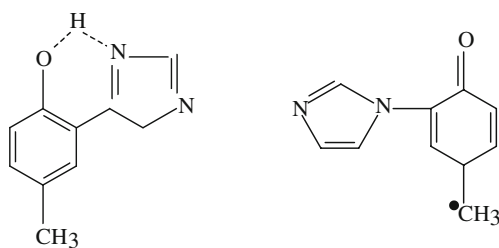


Fig. 5 The fluorescence decay curves of 3×10^{-5} M YH (a) and C I (b), in 20 mM Tris–HCl buffer, pH 7.4; $\lambda_{\text{em}}=320$ nm; NanoLED pulse, $\lambda_{\text{ex}}=295$ nm and random distribution of weighted residuals; resolution 0.056 ns/ch



Scheme 2 The position of H-bond in the C I chemical structure (*left*) and tyrosyl radical formation in the YH compound (*right*)

IR modes of Tyrosyl radical in the YH model compound

To complete the investigation of the Tyr–His model compounds, electrochemically induced FTIR difference spectroscopy was performed. The electrochemically induced FTIR difference spectra are used to identify the interactions and reorganizations of Tyr residues upon electron transfer and coupled proton transfer reactions [29]. We have chosen to study the YH model compound because its chemical structure is closer to that found in proteins like Cytochrome *c* Oxidase. Moreover, the fluorescence emission spectrum of the YH model compound was found to be quite complex, the reason for that deserves to be more investigated. Figure 6 presents the oxidized minus reduced FTIR difference spectrum of the YH model compound for a potential step from 0 to 0.7 V, in 20 mM Tris–HCl pH 7.4. One can observe a very strong stretching mode at $1,717\text{ cm}^{-1}$, attributed to oxidized $\nu(\text{C}=\text{O})$ Tyr. This mode was also observed for redox induced data obtained for free Tyr. Another prominent mode can be observed at $1,598\text{ cm}^{-1}$ which is specific to $\nu(\text{C}-\text{C})$ Tyr ring. Vibrational modes between $1,600$ and $1,560\text{ cm}^{-1}$ are attributed to $\nu(\text{C}-\text{C})$ Tyr ring [29], and the signals at $1,332/1,384\text{ cm}^{-1}$ to the $\nu(\text{C}=\text{C})$ Tyr ring. The contribution at $1,489/1,519$ is assigned to the Tyrosyl radical formation. Berthomieu et al. [30] observed by Resonance Raman and FTIR spectroscopies that the $\nu(\text{C}-\text{O})$ mode at $1,480\text{--}1,515\text{ cm}^{-1}$ is a sensitive marker of the hydrogen bonding status of substituted-phenoxy and Tyrosyl radicals. The modes at $1,000\text{--}1,300\text{ cm}^{-1}$ are attributed to the Tris–HCl buffer. These signals also involve contributions from $\delta(\text{C}-\text{OH})$ modes of Tyr.

The data show that electron transfer and coupled proton transfer accompany Tyrosyl radical formation in the YH model compound, Scheme 2.

Conclusions

Tyr fluorescence is an interesting approach to study protein conformational changes. Here we present optical absorption

and fluorescence spectra of Tyr–His model compounds, at physiological pH. Having in mind these considerations and the results presented, more general conclusions can be drawn regarding the influence of the *para*-substituent at the phenol ring (the methyl substituent for YH and C I Tyr–His model compounds and the H-atom in the case of C II and C III Tyr–His model compounds) as well as the position of the N atom in the imidazole ring.

The positions and the shape modification of the absorption bands as well as the values of the molar extinction coefficient give evidence for the influence of the *para*-substituent at the phenol ring. By the substitution of the H atom (in C II and C III compounds) with a methyl group (in YH and C I compounds) at the phenol ring, a bathochromic shift within the spectra is observed. This fact is attributed to the extent of the conjugation of the π -electrons, corroborated also with the N position in the imidazole ring.

All four investigated Tyr–His model compounds are fluorescent. The fluorescence emission spectra of YH, C I and C II compounds present the same behavior. The fluorescence quantum yield value of C I is higher than the values of the C II and the YH compounds. In the case of the C III compound, the bathochromic shift observed in the fluorescence emission spectrum is more pronounced in comparison with the other compounds. This fact is attributed to the increasing C=N conjugation; The fluorescence quantum yield value of the C III compound is almost two times lower than the value of the C I and the C II compounds. The lifetime value of the C III compound is smaller than that of the other model compounds, meaning that the C III compound is less stable than the others in the excited state.

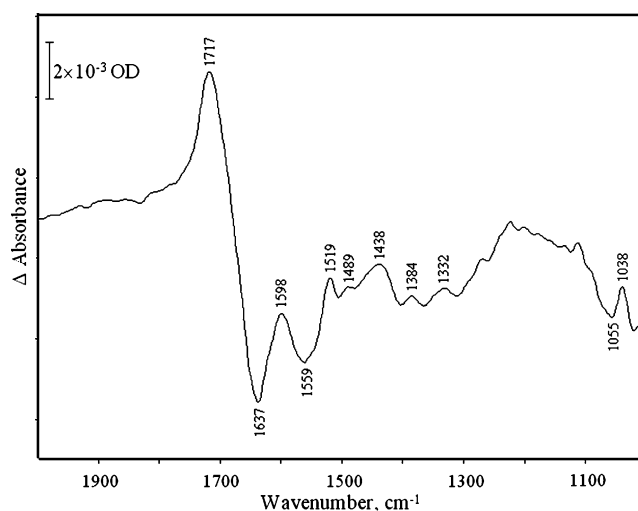


Fig. 6 Oxidized minus reduced FTIR difference spectrum of the YH model compound for the potential step from 0 to 0.7 V (vs. Ag/AgCl/3 M KCl) at pH 7.4

The experimental data obtained clearly demonstrate that the Tyr–His linkage leads to changes in the spectral properties of Tyr. The electrochemically induced FTIR data show that electron transfer and coupled proton transfer accompany Tyrosyl radical formation in the YH model compound. Thus, the presence of Tyr and His residues in a protein leads to the changes in the protein structure, changes that depend on the presence of a Tyr–His linkage.

The fluorescence of Tyr is only slightly quenched in the presence of a covalently attached His and can thus be studied within proteins, like the Cytochrome *c* Oxidase where this linkage is discussed to be crucial for its mechanism.

Acknowledgments This work was supported by CNRS, ULP and ANR. M. Voicescu is grateful for financial support from the CNRS. The authors are indebted to Prof. van der Donk's team, UIUC, Illinois, USA for Tyr–His model compounds synthesis.

References

- Lakowicz JR (1999) Principles of fluorescence spectroscopy, 2nd edn. Kluwer Academic, Dordrecht, pp 448–514
- Ross JBA, Laws WR, Roussland KW, Wyssbrod HR (1992) Tyrosine fluorescence and phosphorescence from proteins and polypeptides. In: Lakowicz JR (ed) Topics in fluorescence spectroscopy, vol. 3. Biochemical applications. Plenum, New York, pp 1–63
- Seidel C, Orth A, Greulich K-O (1993) Electronic effects on the fluorescence of tyrosine in small peptides. Photochem Photobiol 58:178–184 doi:10.1111/j.1751-1097.1993.tb09546.x
- Wiczek W, Rzeska A, Łukomska J, Stachowiak K, Karolczak J, Malicka J et al (2001) Mechanism of fluorescence quenching of tyrosine derivatives by amide group. Chem Phys Lett 341:99–106 doi:10.1016/S0009-2614(01)00470-5
- Łukomska J, Rzeska A, Malicka J, Wiczek W (2001) Influence of substituent on amide nitrogen atom on fluorescence efficiency quenching of Tyr(Me) by amide groups. J Photochem Photobiol Chem 142:135–123 doi:10.1016/S1010-6030(01)00521-4
- White A (1959) Effect of pH on fluorescence of tyrosine, tryptophan and related compounds. Biochem J 71:217–220
- Szabelski M, Guzow K, Rzeska A, Malika J, Przyborowska M, Wiczek W (2002) Acidity of carboxyl group of tyrosine and its analogues and derivatives studied by steady-state fluorescence spectroscopy. J Photochem Photobiol Chem 152:73–78 doi:10.1016/S1010-6030(02)00187-9
- Pal H, Palit DK, Mukherejee T, Mittal P (1990) Some aspects of steady state and time-resolved fluorescence of tyrosine and related compounds. J Photochem Photobiol Chem 52:391–409 doi:10.1016/1010-6030(90)85018-R
- Wilis KJ, Szabo AG (1991) Fluorescence decay kinetics of tyrosinate and tyrosine hydrogen-bonded complexes. J Phys Chem 95:1585–1589 doi:10.1021/j100157a015
- Laws WR, Ross JBA, Wyssbrod HR, Beechem JM, Brand L, Sutherland JC (1986) Time-resolved fluorescence and proton NMR studies of tyrosine and tyrosine analogs: correlation of NMR-determined rotamer populations and fluorescence kinetics. Biochemistry 25:599–607 doi:10.1021/bi00351a013
- Rayner DM, Kraycarski DT, Szabo AG (1978) Excited state acid–base equilibrium of tyrosine. Can J Chem 56:1238–1245 doi:10.1139/v78-206
- Fayet M, Wahl P (1971) Variation avec le pH du rendement quantique et du déclin de la fluorescence de la tyrosine. The variation in the quantum yield and fluorescence decay of tyrosine as a function of pH. Biochim Biophys Acta 221:102–112
- Feitelson J (1964) On the mechanism of fluorescence quenching. Tyrosine and similar compounds. J Phys Chem 68:391–397 doi:10.1021/j100784a033
- Guzow K, Szabelski M, Rzeska A, Karolczak J, Sulowska H, Wiczek W (2002) Photophysical properties of tyrosine at low pH range. Chem Phys Lett 362:519–526 doi:10.1016/S0009-2614(02)01135-1
- Vos R, Engelborghs Y (1994) A Fluorescence study of tryptophan–histidine interactions in the peptide anantin and in solution. Photochem Photobiol 60:24–32
- Pratt DA, Pesavento RP, van der Donk WA (2005) Model studies of the histidine–tyrosine cross link in cytochrome *c* oxidase reveal the flexible substituent effect of the imidazole moiety. Org Lett 7:2735–2738 doi:10.1021/ol050916g
- Parker CA, Rees WT (1960) Corrections of fluorescence spectra and measurement quantum efficiency. Analyst (Lond.) 85:587–600 doi:10.1039/an9608500587
- Chen RF (1967) Fluorescence quantum yields of tryptophan and tyrosine. Anal Lett 1:35–42
- Farinha JPS, Martinho JMG, Pogliani L (1997) Non-linear least-squares and chemical kinetics. An improved method to analyse monomer–excimer decay data. J Math Chem 21:131–139 doi:10.1023/A:1019114217567
- Moss D, Nabedryk E, Breton J, Mantele W (1990) Redox-linked conformational changes in proteins detected by a combination of infrared spectroscopy and protein electrochemistry. Evaluation of the technique with cytochrome *c*. Eur J Biochem 187:565–572 doi:10.1111/j.1432-1033.1990.tb15338.x
- Hellwig P, Behr J, Ostermeier C, Richter OMH, Pfitzner U, Odenwald A et al (1998) Involvement of glutamic acid 278 in the redox reaction of the cytochrome *c* oxidase from *Paracoccus denitrificans* investigated by FTIR spectroscopy. Biochemistry 37:7390–7399 doi:10.1021/bi9725576
- Marques AT, Silva JA, Silva MR, Beja AM, Justino LL, Sobral AJ (2008) X-ray diffraction and DFT studies of 2-methoxy-5-phenylaniline. J Chem Crystallogr 38:295–299 doi:10.1007/s10870-007-9306-6
- Lakowicz JR, Weber G (1973) Quenching of fluorescence by oxygen. A probe for structural fluctuations in macromolecules. Biochemistry 12:4161–4170 doi:10.1021/bi00745a020
- Lakowicz JR, Weber G (1973) Quenching of protein fluorescence by oxygen. Detection of structural fluctuations in proteins in the nanosecond time scale. Biochemistry 12:4171–4179 doi:10.1021/bi00745a021
- Lakowicz JR, Maliwal BP (1983) Oxygen quenching and fluorescence depolarization of tyrosine residues in proteins. J Biol Chem 258:4794–4801
- Shinitzky M, Goldman R (1967) Fluorometric detection of histidine–tryptophan complexes in peptides and proteins. Eur J Biochem 3:139–144 doi:10.1111/j.1432-1033.1967.tb19508.x
- Ross JBA, Laws WR, Buku A, Sutherland JC, Wyssbrod HR (1986) Time-resolved fluorescence and ¹H NMR studies of tyrosyl residues oxytocin and small peptides. Correlation and of NMR determined conformations of tyrosyl residues and fluorescence decay kinetics. Biochemistry 25:607–612 doi:10.1021/bi00351a014
- Guzow K, Ganzynkiewicz R, Rzeska A, Mrozek J, Szabelski M, Karolczak J et al (2004) Photophysical properties of tyrosine and its simple derivatives studies by time-resolved

- fluorescence spectroscopy, global analysis and theoretical calculations. *J Phys Chem B* 108:3879–3889 doi:[10.1021/jp036721c](https://doi.org/10.1021/jp036721c)
29. Hellwig P, Pfitzner U, Behr J, Rost B, Pesavento RP, v Donk W et al (2002) Vibrational modes of tyrosines in cytochrom *c* oxidase from *Paracoccus denitrificans*: FTIR and electrochemical studies on Tyr-D₄-labeled and on Tyr280His and Tyr35Phe mutant enzymes. *Biochemistry* 41:9116–9125 doi:[10.1021/bi012056r](https://doi.org/10.1021/bi012056r)
30. Berthomieu C, Hienerwadel R (2005) Vibrational spectroscopy to study the properties of redox-active tyrosines in photosystem II and other proteins. *Biochim Biophys Acta* 1707:51–66 doi:[10.1016/j.bbabi.2004.03.011](https://doi.org/10.1016/j.bbabi.2004.03.011)